The Nature of Halogen···Halide Synthons: Theoretical and Crystallographic Studies

Firas F. Awwadi,*,† Roger D. Willett,*,† Kirk A. Peterson,† and Brendan Twamley‡

Department of Chemistry, Washington State University, Pullman, Washington 99164, and University Research Office, University of Idaho, Moscow, Idaho 83844

Received: September 17, 2006; In Final Form: December 20, 2006

Two types of halogen···halide synthons are investigated on the basis of theoretical and crystallographic studies; the simple halogen···halide synthons and the charge assisted halogen···halide synthons. The former interactions were investigated theoretically (ab initio) by studying the energy of interaction of a halide anion with a halocarbon species as a function of Y···X^- separation distance and the C−Y···X^- angle in a series of complexes (R−Y···X^-, R = methyl, phenyl, acetyl or pyridyl; Y = F, Cl, Br, or I; X^- = F^-, Cl^-, Br^-, or I^-). The theoretical study of the latter interaction type was investigated in only one system, the $[(4BP)Cl]_2$ dimer, (4BP = 4-bromopyrdinium cation). Crystal structure determinations, to complement the latter theoretical calculations, were performed on 13 *n*-chloropyridinium and *n*-bromopyridinium halide salts ($n = 2-4$). The theoretical and crystallographic studies indicate that these interactions are controlled by electrostatics and are characterized by linear C−Y···X^- angles and separation distances less than the sum of van der Waals radius (r_{vdW}) of the halogen atom and the ionic radii of the halide anion. The strength of these contacts from calculations varies from weak or absent, e.g., $H_3C-Cl\cdots I^-$, to very strong, e.g., HCC−I···F^- (energy of interaction ca. −153 kJ/mol). The strengths of these contacts are influenced by four factors: (a) the type of the halide anion; (b) the type of the halogen atom; (c) the hybridization of the ipso carbon; (d) the nature of the functional groups. The calculations also show that charge assisted halogen···halide synthons have a comparable strength to simple halogen···halide synthons. The nature of these contacts is explained on the basis of an electrostatic model.

Introduction

The field of crystal engineering has been developed through the systematic efforts to design new organic and inorganic materials. One of the main foci of this field is the study of intermolecular interactions and their utilization in supramolecular synthesis.[1] These forces are important, not only due to their role in helping to arrange structural units in the crystalline lattice but also because these forces participate in the physical properties of solid-state materials, e.g., nonlinear optical behavior, magnetic and electric properties, etc.[2] Intermolecular interactions have also been utilized to control solid-state pericyclic reactions, e.g., dimerization and polymerization.[1d,3] The role of hydrogen bonding in controlling structures in a wide variety of materials has long been recognized. More recently, studies have been carried out showing the importance of halogen bonding, e.g., interactions of halogens with other electronegative species.[4]

An important subset of the halogen bonding synthons is those involving interactions between two halogen species. Initially, halogen···halogen contacts (C−Y···Y−C; Y = Cl, Br, and I) were studied using ab initio calculations and investigation of the Cambridge Structural Data base (CSD).[4] Related synthons, halogen···halide interactions, have recently been found to be more directive in comparison to the traditional halogen···halogen synthon.[5] They are characterized by an essentially linear C−Y···X^- angle and an intermolecular halogen···halide distance less than the sum of van der Waals (r_{vdW}) radii. Even halide···halide interactions have been found to be important in magnetic systems, although they do not appear to have any structural directing effects.[6]

CHART 1: Structure of the Modeled Compounds

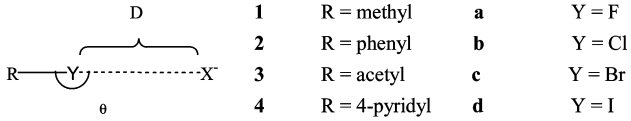

1	R = methyl	**a**	Y = F
2	R = phenyl	**b**	Y = Cl
3	R = acetyl	**c**	Y = Br
4	R = 4-pyridyl	**d**	Y = I

X = F^-, Cl^-, Br^- or I^-

5

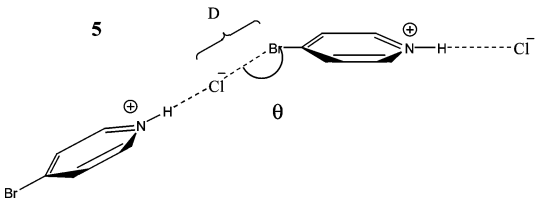

The halogen−halide synthons have been studied crystallographically in several systems to elucidate their role as crystal engineering tools.[5] Many of the systems studied contain halide anions that carry a full negative charge. These studies have been extended by bonding the halide anion to a more electropositive atom (e.g., a metal cation), thereby decreasing the negative charge on the halide, resulting in C−Y···X−M synthons.[7] These interactions play a crucial role in influencing the structures of $(LH)_2MX_4$ and ML_2X_2 compounds (M = Cu(II), Co(II), Pd-

* Corresponding authors. Tel (Office): 509 335 3925. Fax (dept): 509 335 8867. E-mail: fawwadi@yahoo.com (F.F.A.); rdw@mail.wsu.edu (R.D.W.).

† Washington State University.

‡ University of Idaho.

10.1021/jp0660684 CCC: $37.00
Published on Web 03/08/2007

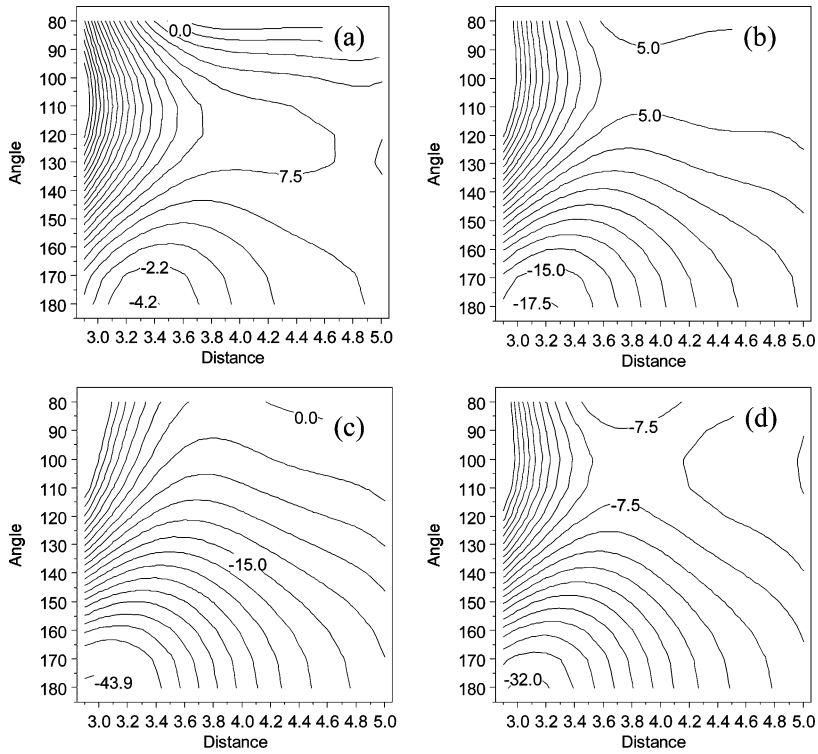

Figure 1. Potential energy diagram for the interaction of a Cl^- anion with (a) bromomethane, **1c**, (b) bromobenzene, **2c**, (c) bromoacetylene, **3c**, and (d) 4-bromopyridine, **4c**, as a function of the C−Br···Cl^- angle, θ, and the Br···Cl^- distance, D. The calculations were performed at dz basis set level. The distances are in angstroms, and the angles are in degrees.

(II), Pt(II); X = F, Cl^-, Br^- or I^-; L = *n*-halopyridine).[7] Yamamoto et al. and others synthesized organic based conducting materials using the halogen···halide synthon.[2] Their study also showed that the synthon was fundamental to the conducting property as well as helping shape the internal architecture of the lattice. Bromine···bromide synthons have been utilized in resolving racemic mixtures of 1,2-dibromohexafluoropropane by crystallizing it with enantiopure trialkylammonium hydrobromides.[2c] More recently, we have used the bromine···bromide synthon to prepare a copper halide decamer, the longest ever known copper halide oligomer.[7c]

Several previous studies initially suggested that these synthonic interactions were a result of HOMO−LUMO charge transfer.[4b] Recently, Zordan et al. showed that the C−Y···X−M synthons involve electrostatic attractions, on the basis of calculated electrostatic potentials.[6e] Their theoretical calculation indicated that the halogen atom in metal halide salts was much more nucleophilic than an organohalogen, but presumably less nucleophilic than a halide ion. Our earlier studies on the C−Br···X−Cu synthonic interactions, and more recent ones on the C−Cl···X−Cu interactions, certainly clearly demonstrate this fact.

In this report, we present theoretical calculations and crystallographic studies on the physical nature of the R−Y···X^- synthons, with a focus on the effect of changing the nature of the R groups.[7f] The theoretical calculations were carried out on two types of R−Y···X^- interactions: (a) First, for the simple R−Y···X^- interactions, the energy of interaction of a halide anion with a halogenated hydrocarbon, was calculated as a function of the separation distance (D) at $\theta = 180°$ for all combinations of R, Y, and X^- (Chart 1). In addition, the θ dependence as a function of D was calculated for the R−Y···X^- synthons (**1cCl**$^-$, **2cCl**$^-$, **3cCl**$^-$, and **4cCl**$^-$). In the aromatic systems (**2cCl**$^-$ and **4cCl**$^-$), the species are assumed to have C_s symmetry and the mirror plane is located in a plane perpendicular to the plane of aromatic ring that bisects the aromatic ring at the bromine atom and the halide anion. (b) Second, the charge assisted halogen···halide interactions were modeled by studying the energy of interaction in the [(4BP)Cl]$_2$ dimer as a function of the distance D at different values of θ. This dimer is also constrained to have C_s symmetry, with the mirror plane bisecting the dimer at the nitrogen and halogen atoms and the halide anions (Chart 1). Crystallographically, the structures of two series of halopyridinium halide salts (*n*CP)X and (*n*BP)X (*n*CP$^+$ = *n*-chloropyridinium; *n*BP$^+$ = *n*-bromopyridinium; $n = 2-4$; X = Cl^-, Br^-, or I^-) were determined to complement the ab initio calculations. The data will indicate that these synthons are controlled by electrostatics.

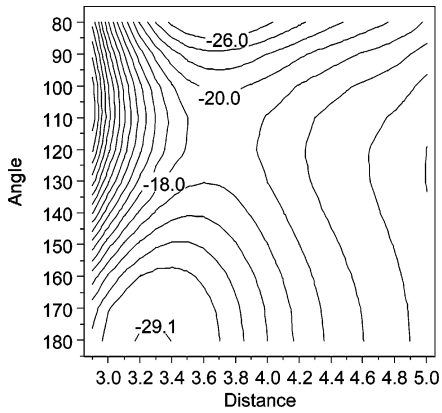

Figure 2. Contour plot of the interaction energy of [(4BP)Cl]$_2$ as function of the C−Br···Cl^- angle, θ, and the Br···Cl^- distance, D. The distances are in angstroms, and the angles are in degrees.

Results

(a) Theoretical Study. The energetics of the interaction of Cl^- ions with organobromine species were carried out both for

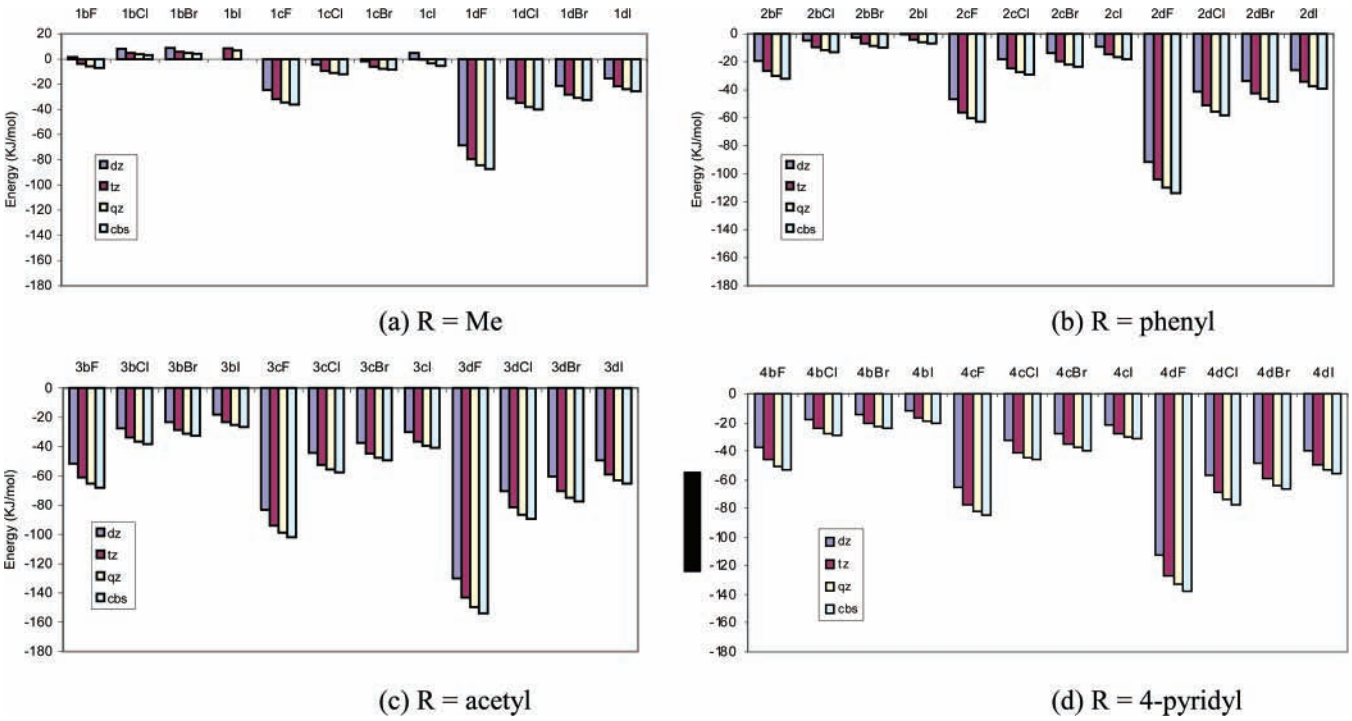

Figure 3. Calculated energy of interaction of halogen···halide synthons for (a) type **1** model compounds, (b) type **2** model compounds, (c) type **3** model compounds, and (d) type **4** model compounds.

TABLE 1: Calculated Separation Distance (Å) at Which the Energy Minima Are Located

	1bF⁻	**1bCl⁻**	**1bBr⁻**	**1bI⁻**	**1cF⁻**	**1cCl⁻**	**1cBr⁻**	**1cI⁻**	**1dF⁻**	**1dCl⁻**	**1dBr⁻**	**1dI⁻**
D_{calc}[a]	2.52	3.28	3.51		2.39	3.11	3.33	3.62	2.33	3.01	3.23	3.49
r_{calc}[b]	85.6	91.9	94.4		74.9	84.7	87.2	89.2	70.8	80.9	82.3	84.0
E_{min}[c]	−7.0	3.0	4.3		−6.3	−12.1	−8.6	−5.5	−7.1	−40.3	−32.5	−5.4
	2bF⁻	**2bCl⁻**	**2bBr⁻**	**2bI⁻**	**2cF⁻**	**2cCl⁻**	**2cBr⁻**	**2cI⁻**	**2dF⁻**	**2dCl⁻**	**2dBr⁻**	**2dI⁻**
D_{calc}[a]	2.39	3.1	3.31	3.6	2.31	3.0	3.21	3.48	2.29	2.94	3.15	3.41
r_{calc}[b]	77.3	86.8	89.0	90.1	72.4	81.7	84.0	85.7	69.6	79.0	80.3	82.0
E_{min}[c]	−32.1	−13.0	−9.9	−6.8	−62.8	−29.0	−23.4	−18.0	−113.6	−58.1	−48.5	−39.3
	3bF⁻	**3bCl⁻**	**3bBr⁻**	**3bI⁻**	**3cF⁻**	**3cCl⁻**	**3cBr⁻**	**3cI⁻**	**3dF⁻**	**3dCl⁻**	**3dBr⁻**	**3dI⁻**
D_{calc}[a]	2.31	2.97	3.17	3.44	2.26	2.91	3.11	3.37	2.28	2.88	3.08	3.39
r_{calc}[b]	74.8	83.2	85.2	86.9	70.8	79.3	81.4	83.0	69.3	77.4	78.6	81.1
E_{min}[c]	−68.0	−38.2	−32.5	−26.6	−101.8	−57.6	−49.4	−40.9	−153.9	−89.5	−77.4	−65.1
	4bF⁻	**4bCl⁻**	**4bBr⁻**	**4bI⁻**	**4cF⁻**	**4cCl⁻**	**4cBr⁻**	**4cI⁻**	**4dF⁻**	**4dCl⁻**	**4dBr⁻**	**4dI⁻**
D_{calc}[a]	2.34	3.03	3.23	3.51	2.28	2.95	3.15	3.42	2.27	2.91	3.11	3.36
r_{calc}[b]	75.7	84.9	86.8	94.7	71.5	80.4	82.5	84.2	68.6	76.8	78.9	80.4
E_{min}[c]	−52.8	−28.9	−24.7	−20.4	−85.0	46.2	−39.5	−32.0	−137.1	−76.9	−66.2	−55.7

[a] Y···X⁻ separation distance at complete basis set level. [b] $r_{calc} = [D_{calc}/(\Sigma r_{vdW}$ of the halogen atom and the ionic radii of the halide anion)] × 100%. [c] The energy is estimated at the complete basis set level.

the ***n*cCl⁻** species ($n = 1-4$) and for $[(4BP)Cl]_2$. The contour plots of the energy of interaction vs the separation distance, D, and angle, θ, show a global energy minimum at $\theta = 180°$ (Figure 1). In addition, for the **2cCl⁻** and **4cCl⁻** species, another smaller minimum at $\theta < 90°$ is observed. For example, in the case of **4cCl⁻**, the minimum energy of −32 kJ/mol occurs at $\theta = 180°$ with $D \sim 3.1$ Å. A saddle point exists in the potential surface at $\theta = 100°$, with energy −7 kJ/mol, which decrease to ca. −8 kJ/mol at $\theta = 90°$ and $D = 3.9$ Å (Figure 1d). These results are in accord with the experimental observations that the short halogen···halide interactions are characterized by the interaction angle of $\theta = 180°$, with much longer contact distances for $\theta \sim 90°$.

Similarly, the contour plot for $[(4BP)Cl]_2$ shows a global energy minimum at $\theta = 180°$ (Figure 2), with energy comparable to that obtained for **4cCl⁻**. Two significant differences exist, however. First, the energy minimum is located at a longer distance in the latter. This indicates the effectiveness of the N−H···Cl⁻ hydrogen bond in removing charge from the chloride ion, increasing the distance and slightly weakening the strength of the C−Br···Cl⁻ interaction. The second difference between the contour plot of **4cCl⁻** (Figure 1d) and $[(4BP)Cl]_2$ (Figure 2) is the increase in the depth of the secondary minimum at $\theta < 90°$ and the decrease in the height of the saddle point. Thus, 90° interactions with distances greater than the sum of the van der Waals and ionic radii are expected to be present in systems involving halopyridinium cations. Because the interactions at $\theta < 90°$ are often influenced by other intermolecular forces that are not part of this discussion (e.g., halide−π interactions,[15] C−H···X⁻, etc), we will not discuss these further.

The calculations indicate that halogen···halide contacts are a result of attractive forces in most of the studied models, with

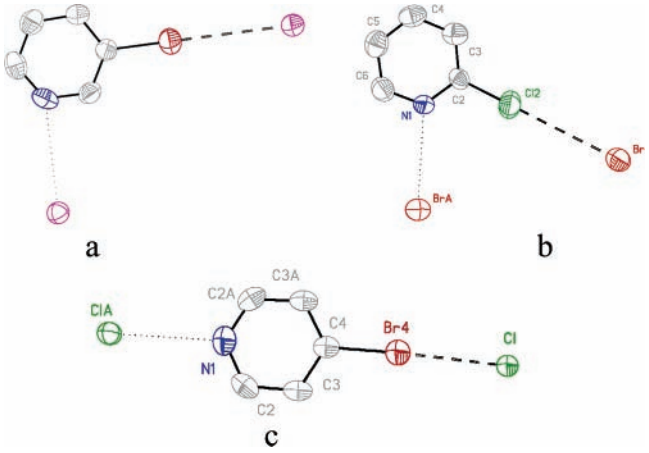

Figure 4. Illustration of the bifunctional nature of the supramolecular interactions in (a) (2CP)Br, (b) (3BP)I, and (c) (4BP)Cl. Hydrogen bonds and halogen−halide synthons are represented by dotted and dashed lines, respectively. Thermal ellipsoids are shown at 50% probability.

several exceptions: the C−F···X$^-$ interactions and the interactions in **1bCl**$^-$, **1bBr**$^-$, and **1cI**$^-$. The halogen···halide interaction strengths in these compounds vary from very weak (**1cI**$^-$, Figure 3a) to very strong (**3dF**$^-$, Figure 3c), on the basis of four main factors: (a) The type of the halide anion. In all of the models the energy of interaction follows the order I$^-$ < Br$^-$ < Cl$^-$ < F$^-$. For example, the energy of interaction in the **2bX**$^-$ series varies from approximately −6.8 kJ/mol for **2bI**$^-$ to −32.1 kJ/mol for **2bF**$^-$ (Figure 3b). (b) The type of the halogen atom. Here, in contrast to halide anions, the energy of interaction follows the order F < Cl < Br < I. In the fluorine−halide case, there is no observed energy minimum for the linear arrangement at the dz basis level. This indicates that no C−F···X$^-$ synthons exist. Similarly, the H_3C−Cl···X$^-$ synthons show no interaction at all basis set levels except for the case of **1bF**$^-$ (Figure 3a). (c) The hybridization of the carbon atom attached to the halogen atom. The strengths of halogen···halide synthons follow the hybridization sp > sp^2 > sp^3. Thus, for **1bF**$^-$, the interaction strength is −7 kJ/mol whereas, in **3bF**$^-$, it is −68 kJ/mol. (d) The nature of the functional groups. Adding an electronegative atom on the organic moiety of the model strengthens the halogen···halide synthon; i.e., replacing the phenyl ring in halobenzene with a pyridyl ring reinforces the strength of the interactions. Thus, in **2bF**$^-$, the energy minimum is −32.1 kJ/mol whereas, in **4bF**$^-$, it is found to be −58.2 kJ/mol.

In all of the models, the separation distance is less than the sum of r_{vdW} of the halogen atom and the ionic radius of the halide anion. This reduction in contact distance is characterized by the parameter r_{calc}, which is defined as

$$r_{calc} = [D_{calc}/(\Sigma r_{vdW} \text{ of the halogen atom and the ionic radii of the halide anion})] \times 100\%$$

(Ionic radii of F$^-$ = 1.33 Å, Cl$^-$ =1.81 Å, Br$^-$ = 1.96 Å, I$^-$ = 2.2 Å. r_{vdW} of Cl = 1.76 Å, Br = 1.86 Å, I = 1.98 Å.) These values are tabulated in Table 1. The r_{calc} value is inversely proportional to the strength of the halogen···halide synthons.

(b) Crystallographic Study. *Structure Descriptions.* Many of the crystal structures in the (*n*YP)X series are isomorphous. To simplify discussion, the structures can be classified into the several structural isomorphous structure sets (Table 2). Each set of structures will be analyzed in the following sequence: (a) examination of the environment around the halide anion to identify the significant C−Y···X$^-$ synthons as well as the classical N−H···X$^-$ hydrogen bonds; (b) description of the resultant supramolecular structures that developed on the basis of these synthons; (c) packing of these supramolecular structures and the resultant three-dimensional structure.

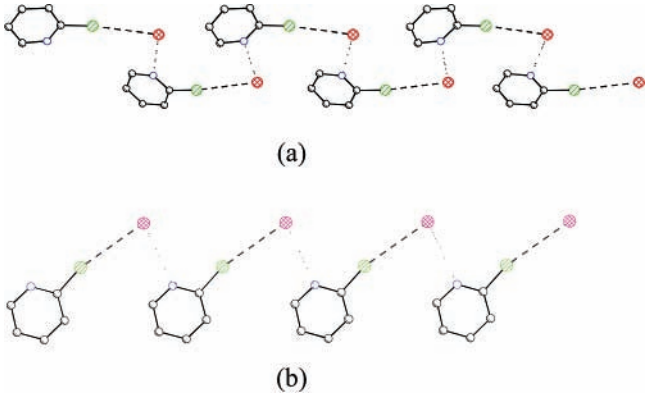

Figure 5. Illustration of the chain networks in (2CP)Br. The chains run parallel to the *c*-axis. Hydrogen bonds and halogen−halide synthons are represented by dotted and dashed lines, respectively.

TABLE 2: Structure Sets for the (*n*CP)X Salts

set	structure type	space group	isomorphous compounds
1	(2CP)Cl[a]	$P2_1/c$	
2	(2CP)Br	$Pca2_1$	(2CP)Br, (2BP)Cl, (2BP)Br, (2BP)I
3	(2CP)I	$P2_1/m$	
4	(3CP)Br	$P\bar{1}$	(3CP)Cl,[a] (3CP)Br, (3BP)Br,[a] (3CP)I, (3BP)Cl
5	(3BP)I	$P2_1/c$	
6	(4CP)Br	$P2_1/m$	(4CP)Br, (4CP)Cl,[b] (4BP)Cl, (4BP)Br[a]
7	(4CP)I	$P\bar{1}$	(4CP)I, (4BP)I

[a] Reference 5a. [b] Reference 5b.

The dominant feature of all of the studied structures, besides the classical N−H···X$^-$ hydrogen bonds, is the presence of the nearly linear C−Y···X$^-$ synthons with a Y···X$^-$ separation distance that is less than sum of r_{vdW} of the halogen atom and the ionic radii of the halide anion. The N−H···X$^-$ hydrogen bonds cooperate with C−Y···X$^-$ synthons to link the halide anions and the halopyridinium cations to form either chain structures or dimers. These chains and dimers aggregate via several secondary synthonic interactions, as discussed below.

C−Y···X$^-$ and N−H···X$^-$ Interactions. The bifunctional nature of the *n*YP$^+$ cations is clearly demonstrated in the (*n*YP)X crystal structures (Figure 4). In all structures, short, nearly linear C−Y···X$^-$ and N−H···X$^-$ contacts exist. Examining the data in Table 3, it is possible to reach several significant conclusions about the nature of the C−Y···X$^-$ synthons. First, by comparing the r_{exp} values, one sees that the C−Br···X$^-$ synthon is significantly stronger than the C−Cl···X$^-$ synthon. Second, in a trend that is not quite as clear (due, primarily, to the different temperatures at which structures were determined), it is seen that the r_{exp} values generally follow the order I < Br < Cl, indicating that the C−Y···X$^-$ synthon is strongest for X$^-$ = I$^-$. This is in contrast to the theoretical results, which predict the opposite trend. However, the theoretical results do not take into account the hydrogen bonding interactions, which are strongest for the chloride salts. From the data in Table 3, it is possible to conclude that the hydrogen bond strength decreases in the order N−H···Cl$^-$ > N−H···Br$^-$ > N−H···I$^-$. The ionic radii increase by 0.15 and 0.44 Å when Cl$^-$ is replaced by Br$^-$ and I$^-$, respectively, whereas the observed increases in the N−H···X$^-$ distances are 0.18 and 0.49 Å, respectively, which are 0.03 and 0.05 Å greater than the increase in ionic radii of

TABLE 3: C−Y···X⁻ and N−H···X⁻ Synthon Distances and Angles in the *n*YP⁺ Salts

compd	Cl···X (Å)	C−Y···X (deg)	N···X (Å)	H···X (Å)	N−H···X (deg)	r_{exp}[a]	Δ*d* (Å)[b]	temp (K)	ref
(2CP)Cl	3.507	164	2.963	1.97	167.0	98.2	0.16	173	5a
(2CP)Br	3.597(4)	170.5(4)	3.139(9)	2.31	163.3	96.7	0.35	298	tw[c]
(2CP)I	3.769(2)	166.8(2)	3.387(5)	2.55	165.2	95.2	0.35	298	tw
(3CP)Cl	3.479	156.1	2.993	2	169.0	97.5	0.19	173	5a
(3CP)Br	3.626(2)	160.3(2)	3.174(6)	2.38	154.3	97.5	0.42	298	tw
(3CP)I	3.739(3)	165.2(3)	3.421(8)	2.63	153.5	94.4	0.43	298	tw
(4CP)Cl	3.335	162.0	2.983	2.11	175.6	93.4	0.3	173	5a
(4CP)Br	3.506(3)	162.6	3.147(8)	2.29	172.6	94.2	0.33	298	tw
(4CP)I	3.733(3)	164.0(3)	3.418(8)	2.60	159.0	94.5	0.4	298	tw
(2BP)Cl	3.310(3)	171.4(2)	2.950(6)	2.11	165.4	90.2	0.3	298	tw
(2BP)Br	3.407(1)	172.4(1)	3.130(4)	2.30	163.3	89.2	0.34	298	tw
(2BP)I	3.575(1)	174.0(1)	3.381(4)	2.55	163.4	88.1	0.35	298	tw
(3BP)Cl	3.359(1)	162.2(1)	2.995(3)	2.20	152.9	91.2	0.39	298	tw
(3BP)Br	3.407	174.3	3.213	2.28	153.0	89.2	0.32	173	5a
(3BP)I	3.589(1)	179.6(2)	3.482(5)	2.74	145.0	88.4	0.54	298	tw
(4BP)Cl	3.313(2)	166.4(2)	3.016(7)	2.16	178.9	90.3	0.35	298	tw
(4BP)Br	3.350	167.4	3.184	2.58	179.9	87.7	0.62	143	5b
(4BP)I	3.648(1)	163.5(3)	3.434(7)	2.63	155.7	89.9	0.43	298	tw

[a] r_{exp} = [(Cl···X distance, exp)/(Σr_{vdW} of the halogen atom and the ionic radius of the halide anion)] × 100%/ [b] Δ*d* = *d*(H···X) − ionic radius of the halide anion. [c] tw denotes "this work".

Figure 6. Chain structures of (4CP)Br in which chains run parallel to the ($\bar{1}$01) direction. Hydrogen bonds and halogen−halide synthons are represented by dotted and dashed lines, respectively.

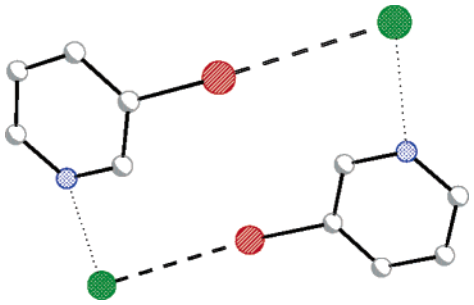

Figure 7. Dimer structures of (3BP)Cl. Hydrogen bonds and halogen−halide synthons are represented by dotted and dashed lines, respectively.

the respective halide ions. These latter interactions are apparently strong enough to counteract the expected trend of the halide ion dependence.

Description of the Supramolecular Networks. Supramolecular networks are built up via the primary N−H···X⁻ and C−Y···X⁻ synthons, in which the halopyridinium cations act as bifunctional supramolecular moieties. In nine of the compounds, these primary synthonic interactions lead to topologically similar chain structures, and in the other four compounds, they lead to the formation of dimeric units. In the (2CP)Br type structures, these chains are generated by a 2-fold screw axis parallel to the *c*-axis (Figure 5) whereas, in the (2CP)I structure, the chains are generated by translation operations parallel to the *a*-axis. The chain structures of the (4YP)X salts have the same connectivity as the chains in the (2YP)X salts, although the differences in geometric nature of the halopyridinium cations yield different structural characteristics, as seen by comparisons of Figures 5 and 6. The chain networks in the (4YP)X compounds are isostructural. In the (4CP)Br type structures, the chain networks run parallel to the ($\bar{1}$01) direction (Figure 6) whereas, in the (4CP)I type structures, the networks run parallel to the (101) direction. In the (3YP)X structures, the presence of the halogen atom at the 3-position makes the formation of the dimer favorable over the chain network (Figure 7). The two bromopyridinium cations of (3BP)I dimer are coplanar; therefore, the dimer has C_{2h} symmetry. In contrast, in (3BP)Cl type structures, the two cations of the dimer are not located in the same plane; hence, this reduces the symmetry to C_i symmetry.

Packing Interactions and Final Crystal Structures. The chains and dimers described in the previous section pack via four different synthons: (a) the N(π)−X⁻ synthon, (b) the N(π)−Y synthon, (c) the C−H···X⁻ synthon, and (d) the C−H···Y synthon. The first two of these synthons exist in 6 of the 7 isomorphous structure sets given in Table 3. These are special cases of more general π−X⁻ and π−Y interactions. However, due to the presence of the electronegative nitrogen atom in the pyridine ring, the shortest halogen and halide contacts with the ring frequently are with the nitrogen atom. The extensive involvement of the C−H moieties in hydrogen bonding can be understood due to the increase in electrostatic potential on the hydrogen atom upon protonation of the pyridine ring (see Figure 10, below).

The N(π)−X⁻ synthons play a major role in the development of the supramolecular structure in the (2YP)X and (4YP)X structures (except for the (2CP)I salt). The N(π)−X⁻ synthons tie the chains in these structures into sheets. This is illustrated in Figure 8a for (4CP)Br, where the N(π)−Br⁻ synthons are shown as the vertical solid lines. These sheets pack via C−H···X⁻ hydrogen bonds in such a way that each halide anion is located between four different cations, due to electrostatic forces, to form the three-dimensional structures, as illustrated in Figure 8b for (4CP)Br. Recently, we found that this pattern of packing to play a significant role in the crystal structures of $(2CP)_2CuX_4$ (X = Cl⁻ and Br⁻).[17]

Both N(π)−X⁻ and N(π)−7 synthons play a role in the development of the supramolecular structure in (3CP)Br type structures. The N(π)−X⁻ synthons link dimers in these structures into double chain or ladder networks that run parallel to the *c*-axis, as illustrated in Figure 9a. Here, alternating N(π)···X⁻

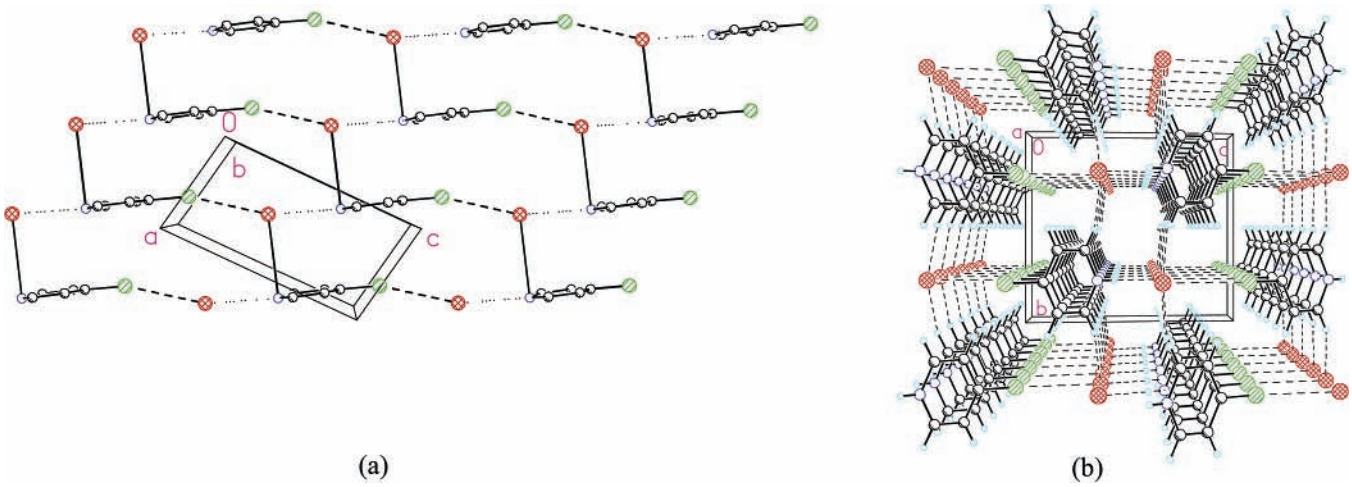

Figure 8. (a) Illustration of the layer structure in (4CP)Br, generated by N(π)−X$^-$ synthons (solid lines) linking the [(4CP)Br]$_n$ chains that run horizontally. Hydrogen bonds and halogen−halide synthons in the chains are represented by dotted and dashed lines, respectively. (b) Illustration of packing of layers into the three-dimensional structures of (4CP)Br. The layers, which lie horizontally in the figure, are linked via C−H···Br$^-$ interactions (dashed vertical lines).

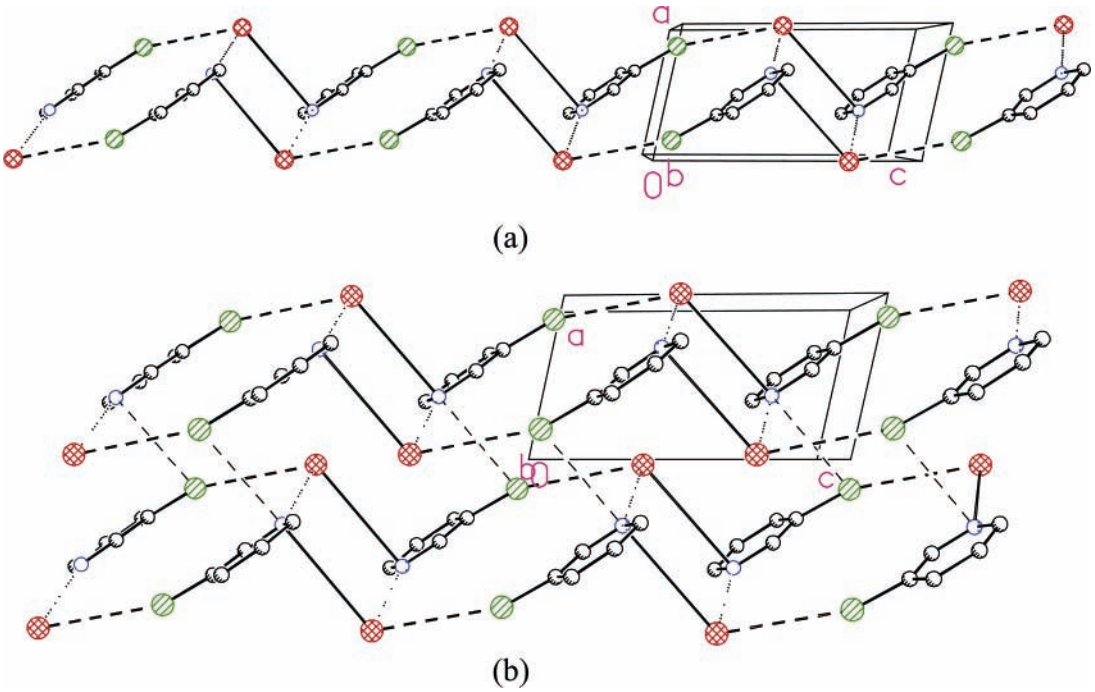

Figure 9. (a) Ladder chain network in (3CP)Br, illustrating the N−H···Br$^-$, C−Cl···Br$^-$, and N(π)−Br$^-$ synthonic interactions. The chains run parallel to the *c*-axis. (b) Illustration of the layer structure of (3CP)Br, showing the N(π)−Cl synthons by dashed lines. The layers lie parallel to the *ac* plane. Hydrogen bonds and halogen−halide, N(π)−Br$^-$, and N(π)−Cl synthons are represented by dotted, thick dashed, solid, and dashed lines, respectively

and C−Y···X$^-$ synthons make up the rails and the N−H···X$^-$ synthons define the rungs. These chains then interact via N(π)−Cl synthons to form a sheet structure that lies in the *ac* plane (Figure 9b). These layers aggregate, on the basis of C−H···X$^-$ hydrogen bonds, in such a manner that each halide anion confronts four chloropyridinium cations. A topologically different double chain structure is developed in the (3BP)I structures. In contrast to the (3CP)Br ladders, alternating N(π)−I$^-$ and N−H···X$^-$ interactions form the rails and the C−Br···I$^-$ interactions form the rungs. Moreover, the N(π)−Y synthons are absent in (3BP)I. Therefore, these chains aggregate to form the three-dimensional structures, based on mainly on C−H···I$^-$ hydrogen bonds.

Further details on the development of the supramolecular structure in these compounds are available in the Supporting Information.

Discussion

The results, both structurally and theoretically, show the significance of the linear C−Y···X$^-$ synthons (Y = Cl, Br, I and X$^-$= F$^-$, Cl$^-$, Br$^-$, I$^-$) in influencing structures of crystalline materials and in use as potential building blocks in crystal engineering via supramolecular synthesis. The strength of these synthons varies from strong forces in **3dF**$^-$ (−153.8 kJ/ mol) to nonexistent in **1bI**$^-$. Calculations indicate that the relative strength of these contacts is influenced by the following four factors: (a) type of the halogen atom; (b) type of the halide anion; (c) hybridization of the ipso carbon relative to the halogen atom; (d) nature of organic moiety attached to the ipso carbon atom.

Halogen···halide interactions, like many other intermolecular interactions, are basically electrostatic in nature. Evidence for

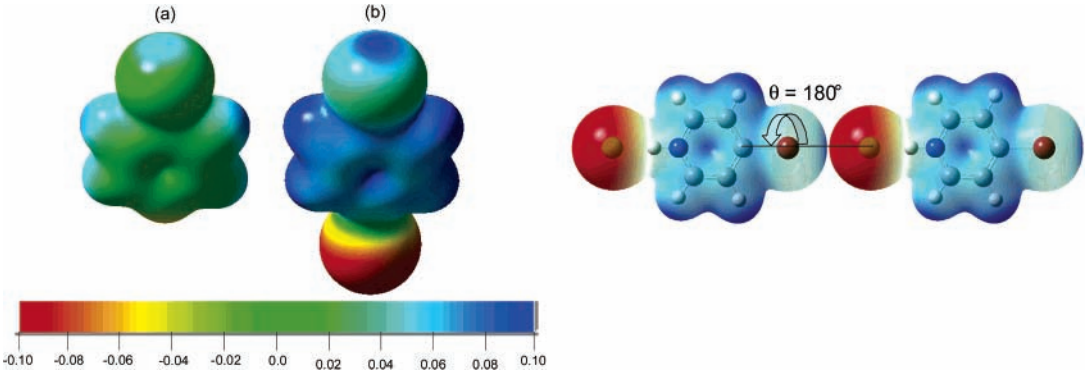

Figure 10. (Left) calculated electrostatic potential of (a) 4-bromopyridine and (b) 4-bromopyridinium chloride. Units of the color scale are in atomic units (energy in hartree and charge in electronic charges). The contour electron density isovalue is set to 0.05. (Right) illustration of the interaction of two 4-bromopyridinium chloride species, showing the linear C−Br···Cl$^-$ geometrical arrangement.

this electrostatic nature will be presented below in the following model, which is based on two main ideas: (a) the presence of a positive electrostatic potential end cap on all halogen atoms except fluorine (Figure 10)[18] and (b) the electron density being anisotropically distributed around the halogen atom.[4c,18a,19] Hence halogen atoms have two radii: a short radius along the C−Y bond and longer one perpendicular to it. According to this model, the halide anion should face the electrostatic potential end cap, and therefore a linear C−Y···X$^-$ geometry is expected. All of the structures in this work display the C−Y···X$^-$ linear arrangement (Table 3). Furthermore, the calculated potential energy diagram shows the presence of an energy minimum at $\theta = 180°$ (Figure 1). Experimentally, the structures presented here cover only one type of halogen···halide contact, C(sp^2)−Y···X$^-$. A search of the Cambridge Structural Data base (CSD),[20] for halogen···halide (F, Cl, Br, and I) intermolecular contacts within the sum of r_{vdW} of the halogen atom and the ionic radius of the halide anion yielded 73 contacts.[21] The data summarizing this information is shown in Table 6. No fluorine···halide or halogen···fluoride contacts have been observed. Contacts of the type C(sp)-Y···X$^-$ were observed only when Y = I.

The calculated energies show that the strength of the C−Y···X$^-$ interaction follows the order I > Br > Cl > F for the halogen Y. The electrostatic model relies on deformation of the electronic charge. Heavier halogen atoms are softer, are less electronegative, and can deform more readily. This agrees with the observed trend in the strength of the C−Y···X$^-$ interaction. Previous calculations have shown that the strength of the electrostatic potential end cap on the halogen follows the same order, I > Br> Cl > F.[18a] Experimentally, this trend is supported by crystallographic data in three different ways: (a) examination of the r_{exp} values, e.g., R−Cl···X$^-$ > R−Br···X$^-$ > R−I···X$^-$, Table 4 (the C(sp^3)−Cl···Cl and C(sp^3)−Br···Cl interactions have almost equal r_{exp} values; however, only two contacts were observed in each case); (b) data showing that when the halogen is changed from F to I, the C−Y···X$^-$ arrangement becomes closer to linearity; (c) competition between C−Y···X$^-$ synthons and N−H···X$^-$ hydrogen bonding in the structures, i.e., where the halogen···halide synthon is stronger, the N−H···X$^-$ hydrogen bond is weaker (Table 3).

The calculations show that the lighter the halide anion, the stronger C−Y···X$^-$ contacts. This is easily described on the basis of the electrostatic model where the smaller anion has higher electron density on the halide anion and therefore stronger attractive electrostatic forces exist. Experimentally, the r_{exp} values show the inverse trend (smallest for iodide salts), which seems to contradict theory. These two trends can be reconciled by taking into account the presence of strong hydrogen bonding (e.g., N−H···X$^-$, for those structures studied in this work), which is also electrostatic in nature.[16] Thus, the strength of the N−H···X$^-$ hydrogen bonding follows the order N−H···Cl$^-$ > N−H···Br$^-$ > N−H···I$^-$. Therefore, due to the competition between halogen···halide contacts and hydrogen bonding, an inverted trend is observed for r_{exp} values (Table 4). This competition also describes why the calculated Y···X$^-$ separation distance at the complete basis set level is always shorter than the experimental value. In a recent study we have shown that C−Cl···Cl−Cu interactions are stronger than those involving C−Cl···Br−Cu synthons, on the basis of the analysis of the structure of (nCP)$_2$CuX$_4$ (nCP$^+$ = n-chloropyridinium; n = 2−4; X = Cl$^-$ or Br$^-$).[17] This analysis showed that C−Cl···Cl−Cu synthons exist in (nCP)$_2$CuCl$_4$, and that the C−Cl···Br−Cu synthon is either absent or very weak in (nCP)$_2$CuBr$_4$.[17] This conclusion supports our results (vide supra).[7f]

TABLE 4: Details of C−Y···X$^-$ Contacts[a]

interaction type	no. of contacts	$\langle r_{exp} \rangle$	θ range (deg)	$\langle q \rangle$
C(sp)−I···Cl$^-$	5	0.81	172.6−179.7	176.4
C(sp)−I···Br$^-$	6	0.82	174.4−178.7	175.7
C(sp^2)−Cl···Cl$^-$	11	0.95	150.0−179.0	163.7
C(sp^2)−Cl···Br$^-$	5	0.97	160.1−172.9	165.3
C(sp^2)−Cl···I$^-$	8	0.95	149.1−174.7	163.8
C(sp^2)−Br···Cl$^-$	11	0.93	156.4−176.4	168.1
C(sp^2)−Br···Br$^-$	11	0.90	156.7−178.1	171.0
C(sp^2)−Br···I$^-$	3	0.89	163.5−179.6	172.4
C(sp^2)−I···Cl$^-$	5	0.87	166.1−173.5	169.9
C(sp^2)−I···Br$^-$	4	0.84	170.1−174.0	173.0
C(sp^2)−I···I$^-$	8	0.83	163.4−178.0	172.9
C(sp^3)−Cl···Cl$^-$	2	0.96	159.1 and 177.3	168.2
C(sp^3)−Br···Cl$^-$	2	0.97	149.0 and 173.3	161.1
C(sp^3)−Br···Br$^-$	2	0.94	164.7 and 169.2	167.0
C(sp^3)−I···I$^-$	3	0.92	166.7−174.0	170.8

[a] Both the data obtained from CSD and the structures reported in this work are used to calculate $\langle r_{exp} \rangle$ and the θ range.

The theoretical calculations show that, as the hybridization of the carbon atom changes from sp^3 to sp, the energy of the interaction increases. The positive electrostatic end cap increases as the hybridization of the carbon atom changes from sp^3 to sp.[18a] This behavior parallels the electronegativity of the carbon atom, which, due to the higher s character, is higher for sp hybridization. Experimentally, given the limited number of data, r_{exp} values support this behavior, and r_{exp} values follow the order C(sp)−Y···X$^-$ < C(sp^2)−Y···X$^-$ < C(sp^3)−Y···X$^-$ (Table 4).

From calculations, replacing the phenyl group with a pyridyl group increases the strength of these contacts. Similarly to the results found for the change in hybridization of the ipso carbon,

TABLE 5: Summary of Data Collection and Refinement Parameters for (*n*CP)X

crystal	(2CP)Br	(2CP)I	(3CP)Br	(3CP)I	(4CP)Br	(4CP)I
formula	C_5H_5BrClN	C_5H_5ClIN	C_5H_5BrClN	C_5H_5ClIN	C_5H_5BrClN	C_5H_5ClIN
formula weight	194.46	241.45	194.46	241.45	194.46	241.45
D_{calc} (mg/m^3)	1.863	2.108	1.879	2.139	1.874	2.090
T (K)	295(2)	295(2)	295(2)	295(2)	295(2)	295(2)
crystal system	orthorhombic	monoclinic	triclinic	triclinic	monoclinic	triclinic
space group	$Pca2_1$	$P2_1/m$	$P\bar{1}$	$P\bar{1}$	$P2_1/m$	$P\bar{1}$
a (Å)	13.782(2)	6.927(2)	4.908(1)	5.128(2)	4.699(1)	5.090(1)
b (Å)	4.700(1)	6.625(2)	7.802(1)	8.224(6)	8.182(2)	8.576(1)
c (Å)	10.707(2)	8.512(2)	9.252(1)	9.276(6)	9.103(2)	9.102(1)
α (deg)	90	90	83.63(1)	83.82(5)	90	83.51(1)
β (deg)	90	103.19(2)	77.59(2)	74.66(5)	100.05(1)	76.39(2)
γ (deg)	90	90	86.92(2)	86.82(6)	90	89.06(2)
V (Å^3)	693.5(2)	380.3(2)	343.7(1)	374.9(4)	344.6(1)	383.7(1)
ind. reflections	702	716	1129	1068	632	1285
R(int)	0.0417	0.0359	0.0431	0.0662	0.0573	0.0327
Z	4	2	2	2	2	2
goodness of fit	1.088	1.083	1.034	1.096	1.065	1.008
R_1[a] [$I > 2\sigma$]	0.0447	0.0306	0.0474	0.0514	0.0445	0.0449
wR_2[b] [$I > 2\sigma$]	0.0868	0.0695	0.1118	0.1279	0.0958	0.0761
μ, mm^{-1}	6.206	4.464	6.260	4.528	6.243	4.425
trans. range	0.190−0.456	0.469−0.469	0.117−0.573	0.344−0.660	0.454−0.574	0.472−0.666

[a] $R_1 = \Sigma||F_o| - |F_c||/\Sigma|F_o|$. [b] $wR_2 = \{\Sigma[w(F_o^2 - F_c^2)^2]/\Sigma[w(F_o^2)^2]\}^{1/2}$.

TABLE 6: Summary of Data Collection and Refinement Parameters for (*n*BP)X

crystal	(2BP)Cl	(2BP)Br	(2BP)I	(3BP)Cl	(3BP)I	(4BP)Cl	(4BP)I
formula	C_5H_5BrClN	$C_5H_5Br_2N$	C_5H_5BrIN	C_5H_5BrClN	C_5H_5BrIN	C_5H_5BrClN	C_5H_5BrIN
formula weight	194.46	238.92	285.91	194.46	285.91	194.46	285.91
D_{calc} (mg/m^3)	1.926	2.247	2.431	1.974	2.478	1.915	2.447
T (K)	297(2)	297(2)	299(2) K	295(2)	295(2)	295(2)	295(2)
crystal system	orthorhombic	orthorhombic	orthorhombic	triclinic	monoclinic	monoclinic	triclinic
space group	$Pca2_1$	$Pca2_1$	$Pca2_1$	$P\bar{1}$	$P2_1/c$	$P2_1/m$	$P\bar{1}$
a (Å)	14.274(3)	14.273(2)	14.504(2)	4.769(1)	4.805(1)	4.392(1)	4.981(1)
b (Å)	4.440(1)	4.601(1)	4.883(1)	7.744(2)	14.391(3)	8.179(2)	8.507(2)
c (Å)	10.581(2)	10.753(2)	11.030(1)	9.153(2)	11.121(2)	9.434(2)	9.453(2)
α (deg)	90	90	90	84.26(3)	90	90	80.18(2)
β (deg)	90	90	90	76.91(3)	94.69(3)	95.83(3)	79.48(2)
γ (deg)	90	90	90	86.06(3)	90	90	88.91(2)
V (Å^3)	670.5(2)	706.2(2)	781.1(2)	327.2(1)	766.4(3)	337.2(1)	388.0(1)
ind. reflections	1538	1434	1721	1493	1263	822	1327
R(int)	0.0631	0.0348	0.0283	0.0337	0.0409	0.0513	0.0395
Z	4	4	4	2	4	2	2
goodness of fit	0.984	1.032	1.029	1.032	1.081	1.104	1.061
R_1[a] [$I > 2\sigma$]	0.0463	0.0282	0.0235	0.0421	0.0320	0.0459	0.0436
wR_2[b] [$I > 2\sigma$]	0.0851	0.0594	0.0475	0.1084	0.0722	0.1078	0.1046
μ, mm^{-1}	6.418	11.374	9.120	6.575	9.295	6.381	9.180
trans. range	0.190−0.724	0.171−0.234	0.164−0.291	0.280−0.779	0.090−0.139	0.251−0.832	0.120−0.460

[a] $R_1 = \Sigma||F_o| - |F_c||/\Sigma|F_o|$. [b] $wR_2 = \{\Sigma[w(F_o^2 - F_c^2)^2]/\Sigma[w(F_o^2)^2]\}^{1/2}$.

adding an electronegative atom to the ipso carbon also increases the electrostatic potential end cap. Recently, we have shown that adding a fluorine atom to the ipso carbon strengthens contacts of the type C−Y···Y−C.[18a] This indicates that as the organic moiety has more electron withdrawing character, a stronger halogen···halide synthon can be predicted.

Calculations show that charge assisted halogen···halide interactions in the dimer $[(4BP)Cl]_2$ are of comparable strength to the simple interaction in **4cCl**$^-$ (Figure 1d and Figure 2). The positive electrostatic potential cap is larger in (4BP)Cl compared to that in 4BP (Figure 8), which is expected to strengthen the halogen···halide synthons. Also, this is expected to be accompanied by a reduction of the negative charge on the chloride anion in (4BP)Cl. In total, both types of interaction are of comparable strengths. However, in the charge assisted halogen···halide interactions, calculations were performed on only one model dimer and the energy minimum in the dimer occurs at a longer distance. This is probably due to competition between the halogen···halide and hydrogen bond synthons.

Several similar intermolecular synthons have been shown to involve attractive electrostatic forces. Zordan et al. have shown that the C−Y···X−M interaction (M = Pt(II) Or Pd(II); X = F, Cl, Br, I) involves electrostatic attraction.[6e] In another study, Lommerse et al. demonstrates that attractive electrostatic forces participate in determining the strength of interaction of C−X···E interactions (X = F, Cl, Br, or I, E = N, O, or S).[22a] The experimental electron density of the molecular aggregation between 4,4′-dipyridyl-*N*,*N*′-dioxide and 1,4-diiodotetrafluorobenzene, and the complex of (*E*)-1,2-bis(4-pyridyl)ethylene with 1,4-diiodotetrafluorobenzene demonstrates that I···O and I···N interactions involve attractive electrostatic forces.[22b,c] These studies support the idea of the presence of an electrostatic potential on the halogen atom (excluding fluorine) in the C−Y bond, and therefore, these synthons involve attractive electrostatic forces.

Conclusions

Both ab initio calculations and crystal structures prove that halogen···halide interactions are controlled by electrostatics and can be used as a crystal engineering tool—deliberately in supramolecular synthesis. These studies show that the interac-

tions are characterized by a linear C−Y···X$^-$ geometry and a Y···X$^-$ separation distance less than the sum of r_{vdW} of the halogen atom and the ionic radii of the halide anion. This geometry is explained by the presence of a positive electrostatic potential end cap on all halogen atoms except fluorine. The strength of these synthons varies from weak or nonexisting (C−F···X$^-$ and H_3C−Cl···X$^-$) to very strong (e.g., **3dF**$^-$, energy of interaction ca. −153 kJ/mol). Four main factors are found to influence the strength of the halogen···halide contacts: (a) the type of halogen atom; (b) the type of the halide anion; (c) the hybridization of the ipso carbon; (d) addition of greater electronegative substituents to the organic group. The calculations also show that charge assisted halogen···halide synthons are of comparable strength to the simple interaction.

Theoretical Method and Experimental Section

(a) Theoretical Method. Gaussian 98 and Gaussian 03[8] were used for geometry optimizations and MOLPRO[9] for single-point energy calculations. For all model compounds (Chart 1), the structure of the molecular unit was optimized using Møller−Plesset second-order perturbation theory (MP2) with a triple-ζ basis set. Similarly, for (4BP)Cl, the geometry was optimized using MP2 and a triple-ζ basis set, with the exception that the N−H distance was constrained to 1.014 Å, the distance obtained by optimizing the geometry of the 4-bromopyridnium cation. The total electronic energy was computed with a series of cc-pVnZ basis sets (aug-cc-pVnZ on Br, Cl, and F, and aug-cc-pVnZ-PP on I, aug = presence of diffuse function on the halogen atom and halide anion) with MP2 (n = D, T, and Q for double-, triple-, and quadruple-ζ, respectively).[10] This involves first Hartree−Fock, self-consistent field calculations to determine the molecular orbitals and then the subsequent MP2 calculation to determine the electron correlation energy. The calculated energy of interaction is corrected for basis set superposition error by the standard counterpoise method.[11] The energy of interaction at the complete basis set limit E(cbs) is estimated using the following equation,[12]

$$E(n) = E(\text{cbs}) + A\text{e}^{-(n-1)} + B\text{e}^{-(n-1)^2}$$

where n = 2 (dz), 3 (tz), 4 (qz) is the cardinal number of the correlation consistent basis set.

(b) Experimental Section. *Synthesis and Crystal Growth.* (a) (2CP)Br, (3CP)Br, (4CP)Br, (2BP)Br, (3BP)Cl, and (4BP)Cl. A general procedure was followed to prepare the above six compounds. Approximately 0.2 g of the base was dissolved in acetonitrile (2 mL). The solution was acidified with concentrated acid (either hydrochloric acid or hydrobromic acid depend on the case). The solution was stirred for 10 min and left for slow evaporation. The next day a crystal with a suitable size for crystal structure determination formed.

(b) (2CP)I. Approximately 0.2 mL of the base was dissolved in 10 mL of ethanol. The solution was acidified with HI. The solution turned yellow, and darkened with time. Colorless crystals formed with a suitable size for X-ray structure determination.

(c) (4CP)I. About 0.2 g of 4-chloropyrdinium chloride was dissolved in 10 mL of absolute ethanol. The solution acidified using concentrated HI. The solution was heated moderately for 1 h and left for slow evaporation. Crystals formed with suitable size for X-ray structure determination.

(d) (3BP)I, (3CP)I, and (2BP)I. About 2 drops of 3-halopyridine was dissolved in 10 mL of methanol. The solution was acidified with HI and left for slow evaporation. Crystals formed with suitable size for X-ray structure determination.

(e) (4BP)I. A small amount of (4BP)Cl was dissolved in methanol. The solution was acidified with HI, heated filtered, and left for slow evaporation.

(f) (2BP)Cl. A 0.2 mL aliquot of 2-bromopyridine was dissolved in 1 mL of propanol. The solution was acidified with concentrated hydrochloric acid (a few drops). The propanol was evaporated under a stream of nitrogen. The solid residue was dissolved in 5 mL of methanol. The solution was left for slow evaporation until crystals of suitable size for X-ray structure determination were formed.

Crystallographic Studies. The diffraction data of the studied compounds were collected at room temperature. The data of the compounds (2CP)Br, (2CP)I, (3CP)Br, (3CP)I, (4CP)Br, (4CP)I, (3BP)I, and (4BP)I were collected on a Syntex $P2_1$ diffractometer upgraded to Bruker $P4$ specifications. The unit cell dimensions were determined from 23−40 accurately centered reflections. The data were collected and reduced using XSCANS 2.20 software.[13] Data were corrected for absorption correction utilizing ψ-scan data, using SHELXTL XPREP software, assuming ellipsoidal shaped crystals.[14d] Data for (2BP)Cl, (2BP)Br, (2BP)I, (3BP)Cl, and (4BP)Cl were collected using a Bruker/Siemens SMART APEX instrument (Mo Kα radiation, λ = 0.710 73 Å). The first 50 frames were recollected at the end of data collection to monitor for decay. Cell parameters were retrieved using SMART software and refined using SAINTPlus on all observed reflections.[14a,b] Data reduction and correction for Lp and decay were performed using the SAINTPlus software.[14b] Absorption corrections were applied using SADABS.[14c] The structures of all compounds were solved by direct methods and refined by the least-squares method on F^2 using the SHELXTL program package.[14d] All non-hydrogen atoms were refined anisotropically. Hydrogen atoms were placed in calculated positions. Details of the data collection and refinement are given in Tables 5 and 6.

Acknowledgment. Work supported in part by ACS-PRF 34779-AC. The Bruker (Siemens) SMART CCD diffraction facility was established at the University of Idaho with the assistance of the NSF-EPSCoR program and the M. J. Murdock Charitable Trust, Vancouver, WA.

Supporting Information Available: Crystal data for all the 13 compounds in CIF format, packing figures, $\pi-\pi$ stacking parameters, and the energy of interaction at various basis set levels. This material is available free of charge via the Internet at http://pubs.acs.org.

References and Notes

(1) (a) Desiraju, G. R. *Nature* **2001**, *412*, 397−400. (b) Desiraju, G. R. *Crystal Engineering: The Design of Organic Solids*; Elsevier Science Publishers B. V.: Amsterdam, 1989. (c) Desiraju, R. G. *Angew. Chem. Int. Ed. Engl.* **1995**, *34*, 2311−2327. (d) Brammer, L. *Chem. Soc. Rev.* **2004**. (e) Braga, D.; Brammer, L.; Champness, N. *Cryst. Eng. Commun.* **2005**, *7*, 1−19.

(2) (a) Yamamoto, H. M.; Yamaura, J.; Kato, R. *J. Am. Chem. Soc.* **1998**, *120*, 5905−5913 and references therein. (b) Domercq, B.; Devic, T.; Fourmigue, M.; Auban-Senzier, P.; Canadell, E. *J. Mater. Chem.* **2001**, *11*, 1570−1575. (c) Farina, A.; Meille, S. V.; Messina, T. M.; Metrangolo, P.; Resnati, G.; Vecchio, G. *Angew. Chem. Int. Ed.* **1999**, *38*, 2433−2436.

(3) (a) Hasegawa, M. *Advances in Physical Organic Chemistry*; Academic Press: London, 1995; Vol. 30, pp 117−171. (b) MacGillivray, L. R.; Reid, J. L.; Ripmeester, J. A. *J. Am. Chem. Soc.* **2000**, *122*, 7817−7818. (c) Matsumoto, A.; Tanaka, T.; Tsubouchi, T.; Tashiro, K.; Saragai, S.; Nakamoto, Sh. *J. Am. Chem. Soc.* **2002**, *124*, 8891−8902.

(4) (a) Desiraju, G. R.; Parthasarathy, R. *J. Am. Chem. Soc.* **1989**, *111*, 8725−8726. (b) Ramasubbu, N.; Parthasarathy, R.; Murray-Rust, P. *J. Am.*

Chem. Soc. **1986**, *108*, 4308−4314. (c) Jagarlapudi, A. R.; Sarma, P.; Desiraju, G. *Acc. Chem. Res.* **1986**, *19*, 222−228. (d) Price, S. L.; Stone, A. J.; Lucas, J.; Rowland, R. S.; Thornley, A. E. *J. Am. Chem. Soc.* **1994**, *116*, 4910−4918.

(5) (a) Freytag, M.; Jones, P. G. *Z. Naturforsch. B: Chem. Sci.* **2001**, *56*, 889−896. (b) Freytag, M.; Jones, P. G.; Ahrens, B.; Fischer, A. K. *New J. Chem.* **1999**, *23*, 1137−1139. (c) Logothetis, Th.; Meyer, F.; Metrangolo, P.; Pilati, T.; Resnati, G. *New. J. Chem.* **2004**, *28*, 760−763. (d) Kuhn, N.; Abu-Rayyan, A.; Eichele, K.; Schwarz, S.; Steimann, M. *Inorg. Chim. Acta* **2004**, *357*, 1799−1804.

(6) (a) Halvorson, K.; Willett, R. D. *Acta Crystallogr.* **1988**, *C44*, 2071. (b) Snively, L. O.; Tuthill, G.; Drumheller, J. E. *Phys. Rev. B* **1981**, *24*, 5349. (c) Block Jansen, R. L. *Phys. Rev. B* **1982**, *26*, 148. (d) Straatman, P.; Block Jenson, R. L. *Phys. Rev. B* **1984**, *29*, 1415. (e) Matsumoto, T.; Miyazaki, Y.; Albrecht, A. S.; Landee, C. P.; Turnbull, M. M.; Sorai, M. *J. Phys. Chem. B* **2000**, *104*, 9993. (f) Patyal, B. R.; Scott, B.; Willett, R D. *Phys. Rev. B* **1990**, *41*, 1657. (g) Watson, B. C.; Kotov, V. N.; Meisel, M. W.; Hall, D. W.; Granoth, G. E.; Montfrooij, W. T.; Nagler, S. E.; Jensen, D. A.; Backov, R.; Petruska, M. A.; Fanucci, G. E.; Talham, D. R. *Phys. Rev. Lett.* **2001**, *86*, 5168. (h) Landee, C. P.; Turnbull, M. M.; Galeriu Giantsidis, C. J.; Woodward, F. M. *Phys. Rev. B, Rapid Commun*. **2001**, *63*, 100402R. (i) Willett, R. D.; Galeriu, C.; Landee, C. P.; Turnbull, M. M.; Twamley, B. *Inorg. Chem*. **2004**, *43*, 3804.

(7) (a) Willett, R. D.; Awwadi, F. F.; Butcher, R.; Haddad, S.; Twamley, B. *Cryst. Growth Des.* **2003**, *3*, 301−311. (b) Brammer, L.; Espallargas, G. M.; Adams, H. *Cryst. Eng. Commun.* **2003**, *5*, 343−345. (c) Haddad, S.; Awwadi, F.; Willett, R. D. *Cryst. Growth Des*. **2003**, *3*, 501−505. (d) Zordan, F.; Brammer, L. *Acta Crystallogr.* **2004**, *B60*, 512−519. (e) Zordan, F.; Brammer, L.; Sherwood, P. *J. Am. Chem. Soc.* **2005**, *127*, 5979−5989. (f) Awwadi, F. F.; Willett, R. D.; Twamley, B. *Cryst. Growth Des.* In press.

(8) Frisch, M. J.; Trucks, G. W.; Schlegel, H. B.; Scuseria, G. E.; Robb, M. A.; Cheeseman, J. R.; Montgomery, J. A., Jr.; Vreven, T.; Kudin, K. N.; Burant, J. C.; Millam, J. M.; Iyengar, S. S.; Tomasi, J.; Barone, V.; Mennucci, B.; Cossi, M.; Scalmani, G.; Rega, N.; Petersson, G. A.; Nakatsuji, H.; Hada, M.; Ehara, M.; Toyota, K.; Fukuda, R.; Hasegawa, J.; Ishida, M.; Nakajima, T.; Honda, Y.; Kitao, O.; Nakai, H.; Klene, M.; Li, X.; Knox, J. E.; Hratchian, H. P.; Cross, J. B.; Bakken, V.; Adamo, C.; Jaramillo, J.; Gomperts, R.; Stratmann, R. E.; Yazyev, O.; Austin, A. J.; Cammi, R.; Pomelli, C.; Ochterski, J. W.; Ayala, P. Y.; Morokuma, K.; Voth, G. A.; Salvador, P.; Dannenberg, J. J.; Zakrzewski, V. G.; Dapprich, S.; Daniels, A. D.; Strain, M. C.; Farkas, O.; Malick, D. K.; Rabuck, A. D.; Raghavachari, K.; Foresman, J. B.; Ortiz, J. V.; Cui, Q.; Baboul, A. G.; Clifford, S.; Cioslowski, J.; Stefanov, B. B.; Liu, G.; Liashenko, A.; Piskorz, P.; Komaromi, I.; Martin, R. L.; Fox, D. J.; Keith, T.; Al-Laham, M. A.; Peng, C. Y.; Nanayakkara, A.; Challacombe, M.; Gill, P. M. W.; Johnson, B.; Chen, W.; Wong, M. W.; Gonzalez, C.; Pople, J. A. *Gaussian 03*, revision C.02; Gaussian, Inc.: Wallingford, CT, 2004. Frisch, M. J.; et al. *Gaussian 98*, revision A.11.2; Gaussian Inc.: Pittsburgh, PA, 1998.

(9) MOLPRO is a package of ab initio programs written by H.-P. Werner and P. J. Knowles: version 2002.6 by R. D. Amos, A. Bernhardsson, A. Berning, P. Celani, D. L. Cooper, M. J. O. Deegan, A. J. Dobbyn, F. Eckert, C. Hampel, G. Hetzer, P. J. Knowles, T. Korona, R. Lindh, A. W. Lloyd, S. J. McNicholas, F. R. Manby, W. Meyer, M. E. Mura, A. Nicklass, P. Palmieri, R. Pitzer, G. Rauhut, M. Schütz, U. Schumann, H. Stoll, A. J. Stone, R. Tarroni, T. Thorsteinsson, H.-J. Werner.

(10) (a) Dunning, T. H., Jr. *J. Chem. Phys.* **1989**, *90*, 1007−1023. (b) Kendall, R. A.; Dunning, T. H., Jr.; Harrison, R. J. *J. Chem. Phys.* **1992**, *96*, 6796−6806. (c) Woon, D. E.; Dunning, T. H., Jr. *J. Chem. Phys.* **1993**, *98*, 1358−1371. (d) Wilson, A. K.; Peterson, K. A.; Woon, D. E.; Dunning, T. H., Jr. *J. Chem. Phys.* **1999**, *110*, 7667−7676. (e) Peterson, K. A.; Figgen, D.; Goll, E.; Stoll, H.; Dolg, M. *J. Chem. Phys.* **2003**, *119*, 11113−11123.

(11) Boys, S. F.; Bernardi, F. *Mol. Phys.* **1970**, *19*, 553.

(12) (a) Peterson, K. A.; Woon, D. E.; Dunning, T. H., Jr. *J. Chem. Phys.* **1994**, *100*, 7410−7415. (b) Feller, D.; Peterson, K. A. *J. Chem. Phys.* **1999**, *110*, 8384−8396.

(13) XSCANS, Version 2.2, Siemens Analytical X-ray Instrument, Inc., Madison, WI.

(14) (a) SMART, v.5.626, Bruker Molecular Analysis Research Tool, Bruker AXS, Madison, WI, 2002. (b) SAINTPlus, v.6.36a, Data Reduction and Correction Program, Bruker AXS, Madison, WI, 2001. (c) SADABS, v.2.01, an empirical absorption correction program, Bruker AXS Inc., Madison, WI, 2001. (d) Sheldrick, G. M. SHELXTL, v.6.10, Structure Determination Software Suite, Bruker AXS Inc., Madison, WI, 2001.

(15) Kim, D.; Tarakeshwar, P.; Kim, S. K. *J. Phys. Chem. A* **2004**, *108*, 1250−1258.

(16) Aakeröy, Chapter B.; Beatty, A. M. *Aust. J. Chem.* **2001**, *54*, 409−421.

(17) (a) Awwadi, F. F.; Willett, R. D.; Twamley, B. *Cryst. Growth Des.* **2006**, *6* (8), 1833−1838. (b) Awwadi, F. F. Ph.D. Thesis, Washington State University, 2005.

(18) (a) Awwadi, F. F.; Willett, R. D.; Peterson K. A.; Twamley, B. *Chem. Eur. J.* **2006**, *12*, 8952−8960. (b) Bosch, E.; Barnes, C. L. *Cryst. Growth Des.* **2002**, *2*, 299−302. (c) Auffinger, P.; Hays, F. A.; Westhof, E.; Ho, P. S. *Proc. Natl. Acad. Sci. U.S.A.* **2004**, *10*, 16789−16794.

(19) Nyburg, S. C.; Faerman, C. H. *Acta Crystallogr*. **1985**, *B41*, 274−279.

(20) CSD, version 5.26, November 2004.

(21) The CSD was searched for halogen···halide contacts in room temperature structures, where the ipso carbon is sp, sp^2, or sp^3 hybridized. Six filters were applied to the searches; only organic compounds, crystallographic R factor <0.1, no errors in the crystal structures, not disordered, not polymeric, and no powder structures. To overcome the electronegativity factor, the search was constrained to the cases were the atoms attached to the ipso carbon, other than the halogen atom involved in the contacts, are either carbon or hydrogen.

(22) (a) Lommerse, J. P.; Anthony, J. S.; Taylor, R.; Allen, F. H. *J. Am. Chem. Soc*. **1996**, *118*, 3108−3116. (b) Bianchi, R.; Forni, A.; Pilati, T. *Acta Crystallogr.* **2004**, *B60*, 559−568. (c) Bianchi, R.; Forni, A.; Pilati, T. *Chem. Eur. J.* **2003**, *9*, 1631−1638.